Inner-Sphere Reorganization Energy of Iron−Sulfur Clusters Studied with Theoretical Methods

Emma Sigfridsson, Mats H. M. Olsson, and Ulf Ryde*

Department of Theoretical Chemistry, Lund University, Chemical Centre, P.O. Box 124, S-221 00 Lund, Sweden

Received July 7, 2000

Models of several types of iron−sulfur clusters (e.g., $Fe_4S_4(SCH_3)_4^{2-/3-/4-}$) have been studied with the density functional B3LYP method and medium-sized basis sets. In a vacuum, the inner-sphere reorganization energies are 40, 76, 40, 62, 43, and 42 kJ/mol for the rubredoxin, [2Fe−2S] ferredoxin, Rieske, [4Fe−4S] ferredoxin, high-potential iron protein, and desulfoferrodoxin models, respectively. The first two types of clusters were also studied in the protein, where the reorganization energy was approximately halved. This change is caused by the numerous $NH\cdots S_{Cys}$ hydrogen bonds to the negatively charged iron−sulfur cluster, giving rise to a polar local environment. The reorganization energy of the iron−sulfur clusters is low because the iron ions retain the same geometry and coordination number in both oxidation states. Cysteine ligands give approximately the same reorganization energy as imidazole, but they have the advantage of stabilizing a lower coordination number and giving more covalent bonds and therefore more effective electron-transfer paths.

Introduction

Iron−sulfur clusters are ubiquitous in biology, being present in all types of organisms from bacteria to higher plants and animals.[1,2] They consist of iron ions surrounded by four sulfur ions, either cysteine thiolate groups or inorganic sulfide ions. Regular clusters with one (rubredoxins), two, three, or four (ferredoxins) iron ions are known, as well as a number of more irregular clusters (occasionally with protein ligands other than cysteine).[3−6] The properties of the six types of sites studied in this paper are summarized in Table 1.

The prime function of the iron−sulfur clusters is electron transfer. Together with cytochromes and blue copper proteins they constitute the most important groups of electron carriers in nature. The reduction potentials of iron sulfur clusters (−700 to +400 mV;[5] all reduction potentials are relative to the standard hydrogen electrode) are in general lower than those of the other two types of electron carriers (−300 to +500 mV for the cytochromes[6,7] and +180 to 1000 mV for the blue copper proteins[8]). However, potentials of the individual sites and proteins vary a lot. During electron transfer, iron alternates between the Fe(II) and Fe(III) states. In general, the iron ions are in the high-spin state, but for the polynuclear sites, they are antiferromagnetically coupled to give a low total spin.[2,5,6,9,10]

According to the semiclassical Marcus theory,[11] the rate of electron transfer is given by

$$k_{ET} = \frac{2\pi}{h}\frac{{H_{DA}}^2}{\sqrt{4\pi\lambda RT}}\exp\left(\frac{-(\Delta G^0+\lambda)^2}{4\lambda RT}\right) \qquad (1)$$

Here, H_{DA} is the electronic coupling matrix element, which depends on the overlap of the wave functions of the two states involved in the reaction, ΔG_0 is the free energy of the reaction (the change in reduction potential), and λ is the reorganization energy (the energy associated with relaxing the geometry of the system after electron transfer). The coupling element depends on the localization of the electron to be transferred and the protein matrix between the two active sites. The reduction potential is a function of the electronic and solvation energies (including both the surrounding protein and solvent) of the two sites. The reorganization energy is normally divided into two parts: inner-sphere (λ_i) and outer-sphere reorganization energy (λ_o), depending on which atoms are relaxed. For a metal-containing protein, the inner-sphere reorganization energy is associated with the structural change of the first coordination sphere, whereas the outer-sphere reorganization energy involves structural changes of the remaining protein as well as the solvent.

Several groups have studied the variation of the reduction potential in various iron−sulfur clusters using theoretical methods.[12−20] For example, it has been shown that the reduction potential of related proteins and mutants can be predicted with reasonable accuracy (average error of 50 mV) if the crystal structure is known.[17] If the structure is not known, the accuracy is worse.[21]

However, no direct estimate of the inner-sphere reorganization energy of iron−sulfur clusters in proteins seems to be available. From a theoretical point of view, the inner-sphere reorganization energy is interesting because it is the only parameter in eq 1 that does not depend on the detailed structure of the surrounding protein. Therefore, accurate calculations of realistic models of the isolated metal centers would allow a general comparison of the various types of electron-transfer proteins and how they have optimized their function.

* To whom correspondence should be addressed. Phone: +46-46-222 45 02. Fax: +46-46-222 45 43. E-mail: Ulf.Ryde@teokem.lu.se.

(1) Palmer, G.; Reedijk, J. *Eur. J. Biochem.* **1991**, *200*, 599.
(2) J. Cowan, A. *Inorganic biochemistry, an introduction*; Wiley-VCH: New York, 1997.
(3) Cammack, R. *Adv. Inorg. Chem.* **1992**, *38*, 281−322.
(4) Matsubara, H.; Saeki, K. *Adv. Inorg. Chem.* **1992**, *38*, 223.
(5) Holm, R. H.; Kennepohl, P.; Solomon, E. I. *Chem. Rev.* **1996**, *96*, 2239−2314.
(6) Fraústo da Silvia, J. J. R.; Williams, R. P. J. *The biological chemistry of the elements*; Clarendon Press: Oxford, 1994.
(7) Zhou, H.-X. *J. Biol. Inorg. Chem.* **1997**, *2*, 109.
(8) Gray, H. B.; Williams, R. J. P.; Malmström, B. G. *J. Biol. Inorg. Chem.* **2000**, *5*, 551−559.
(9) Noodleman, L.; Peng, C. Y.; Case, D. A.; Moesca, J.-M. *Coord. Chem. Rev.* **1995**, *144*, 199.
(10) Noodleman, L.; Case, D. A. *Adv. Inorg. Chem.* **1996**, *38*, 423.
(11) Marcus, R. A.; Sutin, N. *Biochim. Biophys. Acta* **1985**, *811*, 265.

10.1021/ic000752u CCC: $20.00
Published on Web 04/25/2001

Table 1. Chemical Structure, Formal Oxidation States, and Reduction Potential of the Six Iron−Sulfur Clusters Included in This Investigation[5,a]

site	structure	reduced state	oxidized state	reduction potential (mV)
rubredoxin	$FeCys_4$	Fe^{II}	Fe^{III}	−100 to 0
desulfoferrodoxin	$FeCysHis_4$	Fe^{II}	Fe^{III}	240
[2Fe−2S] ferredoxin	$Cys_2FeS_2FeCys_2$	$Fe^{II}Fe^{III}$	$Fe^{III}{}_2$	−450 to −150
Rieske site	$Cys_2FeS_2FeHis_2$	$Fe^{II}Fe^{III}$	$Fe^{III}{}_2$	−100 to +400
[4Fe-4S] ferredoxin	$Cys_4Fe_4S_4$	$Fe^{II}{}_3Fe^{III}$	$Fe^{II}{}_2Fe^{III}{}_2$	−700 to −300
high-potential iron protein	$Cys_4Fe_4S_4$	$Fe^{II}{}_2Fe^{III}{}_2$	$Fe^{II}Fe^{III}{}_3$	+100 to +400

[a] The reduction potentials are relative the standard hydrogen electrode.

Recently, we have published a detailed discussion of the inner-sphere reorganization energy of the blue copper proteins and the related Cu_A dimer (found in cytochrome *c* oxidase and nitrous oxide reductase), both in a vacuum and in the protein.[22−24] To put these results in perspective, we calculate in this paper the inner-sphere reorganization energy of a number of iron−sulfur cluster models. We compare the results with each other and with those of the blue copper proteins and discuss how the various sites have achieved a low reorganization energy.

Methods

Quantum Chemical Geometry Optimizations. Quantum chemical geometry optimizations were performed with the density functional method B3LYP (unrestricted formalism), as implemented in the Turbomole software.[25,26] Hybrid density functional methods have been shown to give as good or better geometries as correlated ab initio methods for first-row transition metal complexes,[27−29] and the B3LYP method in particular seems to give the most reliable results among the widely available density functional methods.[30] In all calculations, we have used for iron the double-ζ basis set of Schäfer et al.[31] (62111111/33111/311), enhanced with one d, one f, and two p functions with exponents 0.1244, 1.339, 0.134 915, and 0.041 843, respectively. For the other atoms, we have employed the 6-31G* basis set.[32] Only the five pure d and seven pure f-type functions were used. Calibrations have shown that geometries obtained with this approach do not change much when the basis set is increased.[33,34] The full geometry of all models was optimized until the change in energy between two iterations was below 10^{-6} hartree (2.6 J/mol) and the norm of the internal gradients was below 10^{-3} au (0.053 pm or 0.057°). Several starting structures were tested to reduce the risk of being trapped in local minima. Only the structures with the lowest energy are reported. No symmetry restraints were imposed.

Six models of iron−sulfur clusters were studied, involving one to four iron ions and zero to four sulfide ions (cf. Table 1). Cysteine ligands were modeled by SCH_3^- and histidine by an imidazole (Im) group. The rubredoxin and desulfoferrodoxin models were assumed to be in the high-spin state (quintet for Fe^{II}, sextet for Fe^{III}), whereas the other models were studied in the open-shell low-spin states (singlet or doublet), obtained from antiferromagnetically coupling of the high-spin state. This is in accordance with experiments[5] and earlier calculations of the electronic structures of the complexes.[9,10] Thus, the oxidized form of the two [2Fe−2S] clusters contained two Fe(III) ions in their high-spin state, antiferromagnetically coupled to an open-shell singlet,[9,10] and the reduced form contained Fe(II) + Fe(III), both in the high-spin state coupled to a doublet.

Similarly, the [4Fe-4S] clusters were treated as two pairs of ferromagnetically coupled high-spin iron ions,[2,5,9] coupled antiferromagnetically together to give a low total spin quantum number. Yet, it should be noted that especially for the reduced cluster, there are several competing electronic states.[9,10] Our study is not intended to exhaustively investigate the electronic structures of these clusters but to give a picture of their reorganization energies compared to those of other iron−sulfur clusters. Therefore, we have only studied one electronic state at each oxidation level, the lowest open-shell singlet or doublet obtained by an antiferromagnetic coupling of the high-spin states. This gives states that are similar (in terms of geometry, spin densities, and charges) to those studied in detail by Noodleman and co-workers.[9,10] More precisely, our $Fe^{II}{}_3Fe^{III}$ state closely corresponds to their OC1 state (i.e., the highest occupied orbital has a σ rather than δ interactions between the reduced iron pair, even if the interaction is far from pure), whereas our Fe^{II}-$Fe^{III}{}_3$ state is close to their OS3 state (i.e., the lowest unoccupied minority spin orbital has iron, rather than sulfur, character).

Reorganization Energies. The inner-sphere reorganization energy was estimated in the same way as for the blue copper proteins.[22] The reorganization energy for the oxidized complex (λ_{ox}) was calculated as the difference in energy between the oxidized complex at its optimal geometry and the reduced complex at the optimal geometry. Likewise, λ_{red} was calculated as the energy of the reduced complex at its optimal geometry minus the energy of the reduced complex calculated at the geometry optimal for the oxidized complex. The total inner-sphere reorganization energy for a self-exchange reaction (λ_i) is the sum of λ_{ox} and λ_{red}. At variance with the outer-sphere reorganization energy, the inner-sphere reorganization energy does not change significantly when a protein docks with its donor or acceptor protein.[35] Therefore, it makes sense to study the inner-sphere reorganization energy of isolated sites without considering their redox partners.

Frequencies were calculated for some of the optimized complexes with the Gaussian 98 software.[36] They were scaled by a factor of 0.963.[37] Force constants for the various bonds, angles, and torsions were calculated from the Hessian matrix using the method of Semi-

(12) Noodleman, L.; Norman, J. G.; Osborne, J. H.; Aizman, A.; Case, D. A. *J. Am. Chem. Soc.* **1985**, *107*, 3418.
(13) Mouesca, J.-M.; Chen, J. L.; Noodleman, L.; Bashford, D.; Case, D. A. *J. Am. Chem. Soc.* **1994**, *116*, 11898.
(14) Noodleman, L. *J. Biol. Inorg. Chem.* **1996**, *1*, 177.
(15) Li, J.; Nelson, M. R.; Peng, C. Y.; Bashford, D.; Noodleman, L. *J. Phys. Chem. A* **1998**, *102*, 6311−6324.
(16) Jensen, G. M.; Warshel, A.; Stephens, P. J. *Biochemistry* **1994**, *33*, 10911.
(17) Stephens, P. J.; Jollie, D. R.; Warshel, A. *Chem. Rev.* **1996**, *96*, 2491.
(18) Swartz, P. D.; Beck, B. W.; Ichiye, T. *Biophys. J.* **1996**, *71*, 2958.
(19) Swartz, P. D.; Ichiye, T. *Biophys. J.* **1997**, *73*, 2733.
(20) Bertini, I. *J. Biol. Inorg. Chem.* **1997**, *2*, 114.
(21) Langen, R.; Warshel, A. *J. Mol. Biol.* **1992**, *224*, 589.
(22) Olsson, M. H. M.; Ryde, U.; Roos, B. O. *Protein Sci.* **1998**, *7*, 2659−2668
(23) Olsson, M. H. M.; Ryde, U. *J. Am. Chem. Soc.*, submitted.
(24) Ryde, U.; Olsson, M. H. M. *Int. J. Quantum Chem.* **2001**, *81*, 335−347.
(25) Treutler, D.; Ahlrich, R. *J. Chem. Phys.* **1995**, *102*, 346.
(26) Hertwig, R. H.; Koch, W. *Chem. Phys. Lett.* **1997**, *268*, 345−351
(27) Ricca, A.; Bauschlicher, C. W. *J. Phys. Chem.* **1994**, *98*, 12899−12903.
(28) Ricca, A.; Bauschlicher, C. W. *Theor. Chim. Acta* **1995**, *92*, 123−131.
(29) Holthausen, M. C.; Mohr, M.; Koch, W. *Chem. Phys. Lett.* **1995**, *240*, 245−252.
(30) Bauschlicher, C. W. *Chem. Phys. Lett.* **1995**, *246*, 40.
(31) Schäfer, A.; Huber, C.; Ahlrichs, R. *J. Chem. Phys.* **1994**, *100*, 5829.
(32) Hehre, W. J.; Radom, L.; Schleyer, P. v. R.; Pople, J. A. In *Ab initio molecular orbital theory*; Wiley-Interscience: New York, 1986.
(33) Ryde, U.; Olsson, M. H. M.; Pierloot, K.; Roos, B. O. *J. Mol. Biol.* **1996**, *261*, 586−596.
(34) Ryde, U.; Olsson, M. H. M.; Carlos Borin, A.; Roos. B. O. *Theor. Chem. Account*, DOI 10.1007/S002140000242.
(35) Ryde, U.; Olsson, M. H. M.; Pierloot, K. The structure and function of blue copper proteins. In *Theoretical Biochemistry: Processes and properties of biological systems*; Eriksson, L., Ed; Elsevier: Amsterdam, 2001; pp 1−56.

nario,[38] which has the advantage of being invariant to the choice of internal coordinates. The force constants were used to calculate approximate contributions to the reorganization energy from various internal distortions:

$$\lambda_j = \sum_b k_b^j (b_{ox} - b_{red})^2 + \sum_\theta k_\theta^j (\theta_{ox} - \theta_{red})^2 + \sum_\varphi \frac{k_\varphi^j}{2}(1 - \cos(n(\varphi_{ox} - \varphi_{red}))) \quad (2)$$

where the three terms represent the energies of bond stretching, angle bending, and dihedral torsions, respectively. b_{ox}, b_{red}, θ_{ox}, θ_{red}, φ_{ox}, and φ_{red} are the bond lengths, angles, and dihedral angles in the optimal oxidized or reduced geometry, respectively, and k_b^j, k_θ^j, and k_φ^j are the corresponding force constants applied to state j, where j is either the oxidized or reduced state.

Spin-Coupling Effects. For the [2Fe−2S] site, we examined the effect of spin coupling on the reorganization energy (the low-spin state is not a pure spin state) using the methods developed by Noodleman and co-workers.[9,13] In essence, the energy of the pure low-spin ground state (E_{ox} and E_{red} in eqs 3−7) is obtained from the low-spin ("broken symmetry") and high-spin energies (E_{BS} and E_{HS}) together with the Heisenberg spin coupling (J_{ox} and J_{red}) and electron delocalization parameters (B), the latter estimated from the energy difference of the orbitals corresponding to the u and g components of the metal d orbitals split by resonance delocalization ($e_{HS,u}$, $e_{HS,g}$).[13] It was hard to identify the correct orbitals in the present systems without symmetry, where the orbitals are far from pure. Therefore, we simply used the HOMO−LUMO gap of the β high-spin orbitals. This gives the smallest possible B factor, which, however, was still too large compared to experimental results (see below). The high-spin wave function was calculated at the same geometry as the low-spin solution. However, we also tested two other conceivable geometries, the optimal high-spin geometry and a symmetrized low-spin geometry (with all Fe−S_i and Fe−S_{Cys} equal to their average in the low-spin geometry).[13] This changed the orbital energy difference by less than 5%. The following relations were used:[15]

$$J_{ox} = 2(E_{HS} - E_{BS})/25 \quad (3)$$

$$E_{ox} = E_{BS} - 5J_{ox}/2 \quad (4)$$

$$B = (e_{HS,u} - e_{HS,g})/10 \quad (5)$$

$$J_{red} = (E_{HS} - E_{BS})/10 + B/2 \quad (6)$$

$$E_{red} = E_{BS} - 2J_{red} \quad (7)$$

Geometry Optimizations in the Protein. For the rubredoxin and [2Fe−2S] ferredoxin sites, geometry optimizations were also performed inside the proteins. These were run with the ComQum-00 program,[24,39] which combines the quantum chemical software Turbomole[25] with molecular mechanical minimizations performed by Amber 5.0.[40] ComQum divides the protein (including solvent) into three subsystems. The central system 1 ($Fe(SCH_3)_4$ or $(SCH_3)_2FeS_2Fe(SCH_3)_2$) was optimized by the B3LYP method. System 2 consisted of all atoms in all amino acids (or solvent molecules) within 1.0 nm of any atom in the quantum system. It was optimized by classical methods. Finally, system 3 comprised the rest of the protein and a cap of water molecules with a radius of 2.4−2.6 nm centered on the geometric center of the protein. System 3 was included in all calculations but was kept fixed at the crystal geometry (an equilibrated conformation for the water cap; crystal waters were kept at the crystal geometry).

In the quantum chemical calculations, system 1 was represented by a wave function, whereas systems 2 and 3 were modeled by an array of point charges, one for each atom, taken from the Amber force-field libraries.[41] Therefore, the polarization of the quantum system by the protein is considered in a self-consistent way. In the classical energy and force calculations, systems 1−3 were represented by the Amber force field[41] but without any electrostatic interactions (which are already treated by quantum mechanics). Special action was taken when there is a bond between the classical and quantum chemical systems (a junction).[39] The quantum chemical system was truncated by hydrogen atoms at the junctions (the C^α of the cysteine ligands), the positions of which were linearly related to the corresponding heavy (typically carbon) atoms in the full system.

The total energy was calculated as

$$E_{tot} = E_{QC} + E_{MM123} - E_{MM1} \quad (8)$$

Here, E_{QC} is the quantum chemical energy of system 1 with H junction atoms, including all the electrostatic interactions. Similarly, E_{MM1} is the classical energy of system 1, still with H junction atoms but without any electrostatic interactions. Finally, E_{MM123} is the classical energy of systems 1−3 with C junction atoms and no electrostatics. This approach is similar to the one used in the Oniom method.[42] The calculated forces are the gradient of this energy, taking into account the variation in the junction atoms.[24]

Optionally, system 2 was optimized by a full molecular mechanics optimization within each cycle of the quantum chemical geometry optimization. In these calculations, systems 1−3 were represented by standard parameters from the classical force field. Electrostatic interactions were included, using Amber charges for systems 2 and 3[41] and quantum chemical charges for system 1.[24]

The reorganization energy in the protein was calculated from the energies of the isolated quantum system only. For calculations with a fixed protein, we could have included also the electrostatic interaction with the protein in the reorganization energies. This changes the individual values of λ_{ox} and λ_{red}, but not their sum, by more than a few kJ/mol.[39] However, for the flexible proteins, this procedure would include a significant amount of the outer-sphere contribution to the reorganization energy and it would give unstable energies. This is caused by the local minima problem. We use a single minimized structure for the calculation of the reorganization energy. However, differences in the hydrogen-bond structure or the positions of the water molecules strongly affect the estimates, and it is impossible to ensure that we have found the global minimum. Moreover, the reorganization energies should be free energies, so they should reflect the dynamics of the system, especially for the solvent molecules. Therefore, direct estimates of the outer-sphere reorganization energy from the ComQum data are not reliable.

(36) Frisch, M. J.; Trucks, G. W.; Schlegel, H. B.; Scuseria, G. E.; Robb, M. A.; Cheeseman, J. R.; Zakrzewski, V. G.; Montgomery, J. A., Jr.; Stratmann, R. E.; Burant, J. C.; Dapprich, S.; Millam, J. M.; Daniels, A. D.; Kudin, K. N.; Strain, M. C.; Farkas, O.; Tomasi, J.; Barone, V.; Cossi, M.; Cammi, R.; Mennucci, B.; Pomelli, C.; Adamo, C.; Clifford, S.; Ochterski, J.; Petersson, G. A.; Ayala, P. Y.; Cui, Q.; Morokuma, K.; Malick, D. K.; Rabuck, A. D.; Raghavachari, K.; Foresman, J. B.; Cioslowski, J.; Ortiz, J. V.; Stefanov, B. B.; Liu, G.; Liashenko, A.; Piskorz, P.; Komaromi, I.; Gomperts, R.; Martin, R. L.; Fox, D. J.; Keith, T.; Al-Laham, M. A.; Peng, C. Y.; Nanayakkara, A.; Gonzalez, C.; Challacombe, M.; Gill, P. M. W.; Johnson, B. G.; Chen, W.; Wong, M. W.; Andres, J. L.; Head-Gordon, M.; Replogle, E. S.; Pople, J. A. *Gaussian 98*, revision A.5; Gaussian, Inc.: Pittsburgh, PA, 1998.
(37) Rahut, G.; Pulay, P. *J. Phys. Chem.* **1995**, *99*, 3093−3100.
(38) Seminario, J. M. *Int. J. Quantum Chem., Quantum Chem. Symp.* **1996**, *30*, 59.
(39) Ryde, U. *J. Comput. Aided Mol. Des.* **1996**, *10*, 153−164.
(40) Case, D. A.; Pearlman, D. A.; Caldwell, J. W.; Cheatham, T. E., III; Ross, W. S.; Simmerling, C. L.; Darden, T. A.; Merz, K. M.; Stanton, R. V.; Cheng, A. L.; Vincent, J. J.; Crowley, M.; Ferguson, D. M.; Radmer, R. J.; Seibel, G. L.; Singh, U. C.; Weiner, P. K.; Kollman, P. A. *Amber*, version 5; University of California, San Francisco, CA, 1997.
(41) Cornell, W. D.; Cieplak, P.; Bayly, C. I.; Gould, I. R.; Merz, K. M., Jr.; Ferguson, D. M.; Spellmeyer, D. C.; Fox, T.; Caldwell, J. W.; Kollman, P. A. *J. Am. Chem. Soc.* **1995**, *117*, 5179−5197.
(42) Svensson, M.; Humbel, S.; Froese, R. D. J.; Matsubara, T.; Sieber, S.; Morokuma, K. *J. Phys. Chem.* **1996**, *100*, 19357.

Table 2. Number of Amino Acids, Water Molecules, and Atoms in Systems 2 and 3 in the ComQum Calculations of Rubredoxin and Ferredoxin

protein	system	residues	water	atoms
rubredoxin, oxidized	2	36	252	1268
	3	16	1340	4237
rubredoxin, reduced	2	36	257	1284
	3	16	1367	4311
ferredoxin	2	54	222	1465
	3	44	1664	5618

The Proteins. The calculations on rubredoxin (from *Desulfovibrio vulgaris*) were based on two crystal structures: the reduced protein at 92 pm resolution and the oxidized protein at 200 pm resolution (Brookhaven Protein Data Bank files 1rb9 and 1rdv, respectively).[43,44] The calculations on [2Fe−2S] ferredoxin were based on the oxidized and reduced crystal structures from Anabaena PCC7119 (130 and 117 pm resolution; PDB files 1qt9 and 1czp, respectively).[45] The proteins were protonated and equilibrated (keeping heavy atoms fixed at the crystal position) together with a water cap (2.4 nm for rubredoxin, 2.6 nm for ferredoxin) in the same way as for the blue copper proteins.[46,47] For residues with multiple conformations, the one with the lower occupancy was ignored, except for residues 45−48 in reduced ferredoxin, where the conformation representative of the reduced site was used (0.4 occupancy). Some water molecules far from the proteins or with low occupancy and close to other atoms were also removed.

On the basis of the solvent accessibility and hydrogen-bond pattern, the two histidine residues in rubredoxin were assumed to be doubly protonated (positively charged). No histidines are present in the ferredoxin. The other amino acids were assumed to be in their normal protonation state at neutral pH, except for the cysteine ligands of the iron sites, which were considered to be deprotonated and negatively charged. The charges of all atoms were taken from the Amber libraries,[41] except for the iron site, which were obtained by quantum chemical calculations. Those of ferredoxin were taken from Noodleman et al.,[9] assuming that the most solvent-exposed iron ion (the one bound to Cys-41 and 46) is the reduced ion. Those of the rubredoxin site were taken from Merz−Kollman calculations[48] on $Fe(SCH_3)_4$, using a large number of potential points (∼40 000). They were 1.209, −0.8434, 0.2200, −0.0594, and 0.0041 e for the Fe, S^{γ}, C^{β}, H^{β}, and C^{α} atoms in the reduced site and 0.8144, −0.5422, 0.0353, 0.0178, and −0.1687 e in the oxidized site. The numbers of amino acids, water molecules, and atoms in each protein are given in Table 2. All calculations were run on IBM SP2, SGI Origin 2000, or Octane workstations.

Results and Discussion

The Rubredoxin Site. First, we studied $Fe(SCH_3)_4^{-/2-}$ as a model of the rubredoxin site. The optimized geometries are set out in Table 3. In the reduced state, all four Fe−S distances are 242 pm. This is longer than the values from experimental structure determinations. For the three most accurate (lowest resolution) crystal structures of reduced proteins in the Brookhaven Protein Data Bank, the average Fe−S distance is 229 pm.[49] Extended X-ray absorption fine structure (EXAFS) measurements give a slightly longer Fe−S bond length, 232 pm.[50] Interestingly, small inorganic model complexes have an even longer Fe−S bond length, 236 pm.[51]

When our $Fe(SCH_3)_4$ model is oxidized, the Fe−S bond lengths decrease to 232 pm (Figure 1). Again, this is longer than those obtained from experiments. The average Fe−S distance in the six most accurate structures of oxidized proteins is 229 pm.[52] This is slightly longer than the EXAFS result of 226 pm[50] and the average Fe−S distance in model compounds, 227 pm.[51]

Thus, we can conclude that our vacuum optimizations give Fe−S bonds that are 5−6 pm longer than those of accurately determined model compounds. However, the *difference* in the Fe−S bond length between the reduced and oxidized structure is well described in our calculations: Our estimate, 10 pm, is very close to the result obtained for inorganic models, 9 pm.[51] Therefore, the calculated reorganization energy, 40 kJ/mol, should be quite accurate.

However, there is a clear difference between the $Fe-S_{Cys}$ bond lengths in inorganic models and in proteins, especially for the reduced model. This is probably an effect of polar interactions in the protein. In the rubredoxins, there are at least six hydrogen bonds between backbone amide groups and the S_{Cys} atoms.[53] A detailed study of the analogous $ZnCys_4^{2-}$ cluster in alcohol dehydrogenase showed that such hydrogen bonds decrease the Zn−S distances by ∼7 pm.[54]

Therefore, we ran a series of geometry optimizations of the rubredoxin cluster in the protein, using the combined quantum chemical and molecular mechanical program ComQum-00.[24,39] Two crystal structures were used (one oxidized, one reduced).[43,44] For each protein, two calculations at each oxidation state were run, one with the protein fixed at the crystal structure and one where the protein was allowed to relax. The results in Table 3 show that the average $Fe-S_{Cys}$ bond length in the protein (237 pm) is 5 pm shorter than in a vacuum for the reduced complex. This is 5 pm longer than the EXAFS value,[50] reflecting a systematic error of the B3LYP method.[33,34] The variation among the four calculations is quite small, ∼1 pm, showing that the results are reliable.

For the oxidized complex, the $Fe-S_{Cys}$ bonds are only 2 pm shorter in the protein (231 pm) than in a vacuum. Again, this is 6 pm longer than the EXAFS results.[5,50,55] Therefore, the change in the $Fe-S_{Cys}$ bond length upon oxidation is very well reproduced, giving confidence in the calculated reorganization energies, presented in Table 4. It can be seen that these energies vary quite substantially among the various calculations (11−35 kJ/mol, average 22 kJ/mol), but all are smaller than the vacuum value (40 kJ/mol). Thus, we can conclude that the dielectric surroundings of the iron site reduce the reorganization energy by almost a factor of 2. The reason for this effect is that the isolated iron site has a high charge, −2 in the reduced state and −1 in the oxidized state. $NH-S_{Cys}$ hydrogen bonds in the protein solvate this charge, but more for the reduced than the oxidized state. This explains why the change is larger for the reduced state.

The inner-sphere reorganization energy of rubredoxin has been estimated to be 22−26 kJ/mol from the change in the Fe−

(43) Dauter, Z.; Butterworth, S.; Sieker, L. C.; Sheldrick, G.; Wilson, K. S. Brookhaven Protein Data Bank, structure 1rb9, 1997.
(44) Misaki, S.; Morimoto, Y.; Ogata, M.; Yagi, T.; Higuchi, Y.; Yasuoka, N. *Acta Crystallogr.* **1999**, *D55*, 408.
(45) Morales, R.; Chron, M.-H.; Hudry-Clergeon, G.; Pétillot, Y.; Norager, S.; Medina, M.; Frey, M. *Biochemistry* **1999**, *38*, 15764.
(46) Pierloot, K.; De Kerpel, J. O. A.; Ryde, U.; Roos, B. O. *J. Am. Chem. Soc.* **1997**, *119*, 218−226.
(47) Pierloot, K.; De Kerpel, J. O. A.; Ryde, U.; Olsson, M. H. M.; Roos, B. O. *J. Am. Chem. Soc.* **1998**, *120*, 13156−13166
(48) Besler, B. H.; Merz, K. M.; Kollman, P. A. *J. Comput. Chem.* **1990**, *11*, 431.
(49) Brookhaven Protein Data Bank files: 1cad, arb9, and 8rxn.
(50) Shulman, R. G.; Eisenberger, P.; Teo, B. K.; Kincaid, B. M.; Brown, G. S. *J. Mol. Biol.* **1978**, *124*, 305.
(51) Lane, R. W.; Ibers, J. A.; Rankel, R. B.; Papaefthymiou, G. C.; Holm, R. H. *J. Am. Chem. Soc.* **1975**, *99*, 84.
(52) Brookhaven Protein Data Bank files: 1caa, 1dfx, 1rdg, 4rxn, 5rxn, and 6rxn.
(53) Adman, E. T.; Watenpaugh, K. D.; Jensen, L. H. *Proc. Natl. Acad. Sci. U.S.A.* **1975**, *72*, 4854−4858.
(54) Ryde, U. *Eur. J. Biophys.* **1996**, *24*, 213−221.
(55) Lippard, S. J.; Berg, J. M. *Principles of bioinorganic chemistry*; University Science Books: Mill Valley, CA, 1994.

Table 3. Optimized Fe−S_{Cys} Distances for the Rubredoxin Model ($Fe(SCH_3)_4$) in Vacuum and Calculated in the Protein with ComQum[24,39,a]

			distance to Fe (pm)				
oxidation state	system	ΔE_1, kJ/mol	S_1	S_2	S_3	S_4	$S_{average}$
II	vacuum		242	242	242	242	242.3
	reduced protein fixed	20.6	234	238	236	238	236.2
	reduced protein flexible	18.1	236	238	238	236	236.7
	oxidized protein fixed	27.4	234	241	237	239	237.7
	oxidized protein flexible	37.2	237	238	239	240	238.5
	models			232−238			236
	protein crystals			224−236			229
	protein EXAFS						232
III	vacuum		232	232	232	232	232.4
	reduced protein fixed	25.0	229	233	228	232	231.0
	reduced protein flexible	36.6	228	232	231	233	230.9
	oxidized protein fixed	15.9	229	231	229	231	230.1
	oxidized protein flexible	14.1	231	229	230	230	230.2
	models			225−228			227
	protein crystals			223−233			229
	protein EXAFS						226

[a] For the latter calculations, it is indicated what protein structure has been used (oxidized or reduced[43,44]) and whether system 2 was allowed to relax or not (flexible or fixed). ΔE_1 is the energy difference (calculated in a vacuum) of system 1 between the vacuum and ComQum geometries. Experimental data from model compounds[51] and proteins (both crystal structures[52,87] and EXAFS data[5,50,55]) are also included.

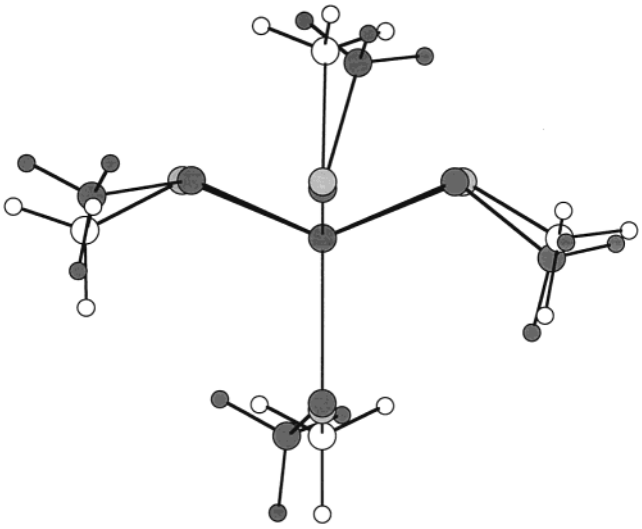

Figure 1. Difference in geometry between the reduced and oxidized (shaded) forms of the rubredoxin model $Fe(SCH_3)_4$.

Table 4. Inner-Sphere Reorganization Energies (kJ/mol) for the Rubredoxin Model ($Fe(SCH_3)_4$) Calculated in Vacuum and in the Protein with ComQum[a]

system	λ_{red}	λ_{ox}	λ_i
vacuum	21.4	18.3	39.7
reduced protein fixed	15.9	8.2	24.1
reduced protein flexible	6.7	4.0	10.7
oxidized protein fixed	14.4	3.2	17.6
oxidized protein flexible	19.0	16.1	35.1

[a] For the latter calculations, it is indicated what protein structure has been used (oxidized or reduced[43,44]) and whether system 2 was allowed to relax or not (flexible or fixed).

S_{Cys} distances in EXAFS experiments (6 pm) combined with the corresponding vibrational frequency.[56,57] This is close to our estimates. In fact, a harmonic analysis based on the calculated Hessian matrix and the geometry change during reduction in a vacuum shows that the Fe−S_{Cys} bonds give the major contribution to the reorganization energy, in total ∼20 kJ/mol. Other bond lengths contribute by less than 1 kJ/mol and the angles by less than 6 kJ/mol (dominated by the S−Fe−S angles). The contribution from the dihedral angles is larger, but for these, the simple approximation in eq 2 breaks down (their sum is much larger than the total reorganization energy). However, it is clear that our calculated reorganization energy is more accurate than estimates from vibrational frequencies because we consider all degrees of freedom and not only the four Fe−S_{Cys} bonds.

Desulforedoxins and the S−Fe−S Angle. The S−Fe−S angles in our optimized models are 109−110° for the reduced and 106−112° for the oxidized model. The larger variation in the latter model is due to stronger hydrogen bonds between the methyl groups and the thiolate ions (cf. Figure 1). The angle is 104−115° in inorganic models.[51] Most rubredoxins have a similar variation in the S−Fe−S angles, 104−117°.

However, in the desulforedoxins, a group of rubredoxins from the bacteria *Desulfovibrio*, the variation is appreciably larger, 103−122°.[58] The reason for this is that two of the cysteine ligands come directly after each other in the sequence (Cys-28 and Cys-29), which for steric reasons gives rise to the largest angle. This has been taken as evidence that the site is in an entatic state,[58] i.e., a state strained by the protein to give a catalytic advantage.

To test this suggestion, we optimized the geometry of the rubredoxin model with one of the S−Fe−S angles constrained to 121.8° as in desulforedoxin.[58] This increased the energy of the complex, but only by 3 kJ/mol in both the reduced and oxidized states. Thus, the strain is very small in energy terms. Moreover, the calculated reorganization energy of the constrained complex is 4 kJ/mol *higher* than for the unconstrained complex, so the constraint does not enhance the rate of electron transfer. Similarly, the reduction potential is unlikely to change significantly because the energy of reduced and oxidized forms increased by the same amount when constrained. Therefore, it seems that this larger angle, which undoubtedly is caused by the folding of the protein, does not affect the properties of the iron−sulfur site in any significant way.

This analysis shows that a large difference in a geometric parameter between two protein structures does not necessarily

(56) Lowery, M. D.; Guckert, J. A.; Gebhard, M. S.; Solomon, E. I. *J. Am. Chem. Soc.* **1993**, *115*, 3012.
(57) Reynolds, J. G.; Coyle, C. L.; Holm, R. H. *J. Am. Chem. Soc.* **1980**, *102*, 4350−4355.
(58) Archer, M.; Carvalho, A. L.; Teixeira, S.; Moura, I.; Moura, J. J. G.; Rusnak, F.; Romão, M. J. *Protein Sci.* **1999**, *8*, 1536.

Table 5. Optimized Geometries for the [2Fe−2S] Ferredoxin Model $(SCH_3)_2FeS_2Fe(SCH_3)_2$ in Vacuum and Calculated in the Protein with the ComQum Program[24,39,a]

			distance to Fe (pm)				
			$Fe-S_{Cys}$		$Fe-S_i$		
oxidation state	system	ΔE_1, kJ/mol	range	av	range	av	Fe−Fe
II + III	vacuum		245−249	247.4	225−241	233.0	299
	reduced protein	92.5	234−243	239.0	225−241	233.0	301
	oxidized protein	54.6	234−240	237.5	221−246	231.6	289
	protein crystals		230−236	232	218−229	224	275
	protein EXAFS				224		276
	vacuum, high spin		247−248	248	230−237	233.2	280
III + III	vacuum		235−237	236.4	226−227	226.5	285
	reduced protein	42.6	230−234	232.1	223−231	226.5	283
	oxidized protein	110.5	228−238	233.8	226−233	228.4	302
	models		230−233	232	219−223	221	267−270
	protein crystals		222−237	229	211−228	221	260−278
	protein EXAFS				223		270−273
	vacuum, high spin		235−237	236.2	230−233	231.6	304

[a] For the latter calculations, it is indicated what protein structure has been used (oxidized or reduced[45]). All calculations were run with a fixed system 2. ΔE_1 is the energy difference (calculated in a vacuum) of system 1 between the vacuum and ComQum geometries. In vacuum, a set of calculations of the high-spin state are also presented. Experimental data from model compounds[61,62] and proteins (both crystal structures[45,63] and EXAFS data[64]) are also included.

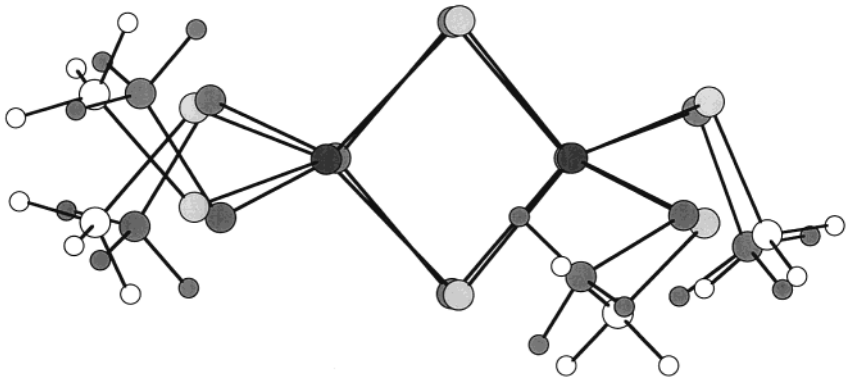

Figure 2. Difference in geometry between the mixed-valence and oxidized (shaded) forms of the [2Fe−2S] ferredoxin model $(SCH_3)_2FeS_2Fe(SCH_3)_2$.

imply any relationship to the function of the site; instead, it may reflect a small force constant (the bond or angle is flexible) so that the difference in energy terms is small and therefore of minor functional importance. Similar results have been obtained for axial interactions in blue copper proteins and Cu_A.[23,59,60]

[2Fe−2S] Ferredoxin Site. Next, we studied $(SCH_3)_2FeS_2Fe(SCH_3)_2$ as a model of the [2Fe−2S] ferredoxins. The optimized structures are described in Table 5. The Fe−Fe distance in the oxidized site is 285 pm, while the $Fe-S_i$ distances are 226−227 pm and the $Fe-S_{Cys}$ distances 235−237 pm (S_i denotes an inorganic sulfide ion). The variation in the Fe−S distances is caused by hydrogen bonds between the methyl groups and the sulfur ions (cf. Figure 2). The Fe−S distances are 4−7 pm longer than in model compounds and protein crystal structures.[61−63] Similarly, the calculated Fe−Fe distances seem to be ∼15 pm too long. However, as can be seen in Figure 3, the Fe−Fe potential energy surface is quite flat: A 15 pm difference corresponds to a change in energy of only ∼5 kJ/mol. Moreover, spin coupling effects (see below) tend to shorten this distance by at least 4 pm.

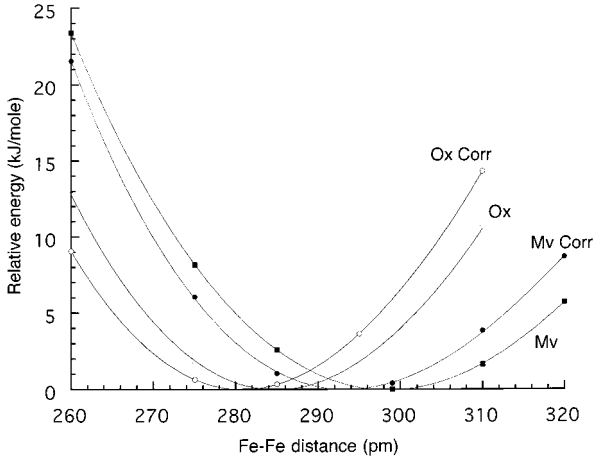

Figure 3. Potential surface of the Fe−Fe interaction in the mixed-valence (Mv) and oxidized (Ox) state of $(SCH_3)_2FeS_2Fe(SCH_3)_2$. Energies are given for both the broken-symmetry solution (for which the geometry was fully optimized in each step) and the corrected pure-spin ground state (Corr).

When the model is reduced, the $Fe-S_{Cys}$ and Fe−Fe distances become 9−12 and 14 pm longer, respectively (Figure 2). The $Fe-S_i$ distances to one of the iron ions increase by 15 pm, whereas those to the other ion decrease by 2 pm. Thus, they become quite dissimilar, 241 and ∼225 pm. This shows that the added electron is localized on one iron atom (the one with

(59) Ryde, U.; Olsson, M. H. M.; Roos, B. O.; De Kerpel, J. O. A.; Pierloot, K. *J. Biol. Inorg. Chem.* **2000**, *5*, 565−574.
(60) Olsson, M. H. M.; Ryde, U. *J. Biol. Inorg. Chem.* **1999**, *4*, 654−663.
(61) Mayerle, J. J.; Denmark, S. E.; DePamphilis, B. V.; Ibers, J. A.; Holm, R. H. *J. Am. Chem. Soc.* **1975**, *97*, 1032.
(62) Ueyama, N.; Yamada, Y.; Okamura, T.-A.; Kimura, S.; Nakamura, A. *Inorg. Chem.* **1996**, *35*, 6473−6484.
(63) Brookhaven Protein Data Bank files: 1frd, 1frr, 1fxi, 1qt9, and 4fxc.

the longer bonds). However, it is also strongly delocalized over the neighboring sulfur ions.

No binuclear inorganic models in the reduced state seem to exist.[55] However, the first crystal structure of a reduced [2Fe−2S] site in a protein was recently published.[45] It does not show the same asymmetry as our structures. This is because the unpaired electron alternates between the two iron sites during the data collection.[55] EXAFS data are also available,[64] but they do not distinguish between the two types of Fe−S bonds. Yet, it is clear that our calculated Fe−S and Fe−Fe distances are longer than those in the proteins. Moreover, the experimental structures show a smaller decrease in the Fe−S distance upon reduction in the protein (1−3 pm) than in our calculations (9 pm). This is not surprising because ∼60% of the iron−sulfur sites in the crystal are oxidized,[45] giving rise to multiple conformations that are hard to discern.

The calculated reorganization energy of our model in a vacuum is quite large, 76 kJ/mol, almost twice as much as for the rubredoxin model. This is in accordance with a lower rate of electron transfer for the [2Fe−2S] sites in proteins as well as in model systems.[55,61] The increase can be rationalized by a detailed study of the change in bond lengths and force constants of the two models. In the dimer, the reduction is mainly confined to one of the iron ions. The changes in the bond lengths upon reduction of this iron ion are slightly larger than for the rubredoxin monomer (on average 13 pm compared to 9 pm). However, there are also appreciable changes around the other iron ion (6 pm on average). The $Fe-S_{Cys}$ force constants are slightly lower in the dimeric site (0.017 compared to ∼0.015 kJ mol^{-1} pm^{-2} in the reduced site and 0.032 compared to ∼0.026 kJ mol^{-1} pm^{-2} in the oxidized site), but those of the $Fe-S_i$ bonds (which are not present in the monomer) are larger (0.027 and 0.039 kJ mol^{-1} pm^{-2}). Therefore, the total reorganization energy of the ferredoxin model is almost doubled. At first, the increase in reorganization energy for the dimeric iron−sulfur clusters may seem strange, considering that the reorganization energy of the dimeric Cu_A site was found to be appreciably *lower* than for the blue-copper monomer (43 kJ/mol compared to 62 kJ/mol). However, the reason for this difference is that the unpaired electron in the mixed-valence Cu_A site is delocalized over the two copper ions.[23,65,66] As suggested by Larsson and co-workers[67] and confirmed by detailed calculations,[23] such delocalization of an electron over two monomers reduces both the bond length change and the force constants of the site, leading to a reduction of the reorganization energy.

It is clear that there are significant differences between the calculated and experimental structure of the reduced site. Considering the results for the rubredoxins, an important reason for this discrepancy may be solvation effects in the protein. The isolated site has a charge of −3, which is larger than for the reduced rubredoxin site (−2). Therefore, we also ran a series of ComQum calculations of the [2Fe−2S] ferredoxins in the protein. Again, we used crystal structures for both reduced and oxidized sites, but the protein was kept rigid in all calculations.

Table 6. Inner-Sphere Reorganization Energies (kJ/mol) for the [2Fe−2S] Ferredoxin Model $(SCH_3)_2FeS_2Fe(SCH_3)_2$ Calculated in Vacuum and in the Protein with ComQum[a]

protein	λ_{red}	λ_{ox}	λ_i
vacuum	34.3 (35.5)	41.5 (44.7)	75.8 (80.2)
reduced protein	44.7 (50.6)	6.9 (7.9)	51.9 (58.5)
oxidized protein	29.0 (17.2)	7.8 (9.8)	36.8 (27.0)
vacuum, high spin	25.5	33.5	59.0

[a] For the latter calculations, it is indicated what protein structure has been used (oxidized or reduced[45]). Reorganization energies have been calculated both directly from the low-spin ("broken-symmetry") energies and from the energies of the pure-spin state extrapolated from the broken-symmetry and high-spin solutions (the latter in parentheses). Data for the high-spin vacuum structure are also given.

The results of these calculations are gathered in Table 5. As for rubredoxin, the $Fe-S_{Cys}$ bond lengths are shortened in the protein by 9 pm in the reduced site and by 3 pm in the oxidized site. These changes are larger than for the rubredoxins, reflecting the larger net charge of the binuclear sites. Interestingly, the $Fe-S_i$ bond lengths do not change significantly in the protein, but the variation increases slightly. The Fe−Fe distance varies quite substantially in the calculations but without any clear trend. This probably reflects the flexibility of the bond (cf. Figure 3).

Consequently, our optimizations in the protein predict that the average $Fe-S_{Cys}$ and $Fe-S_i$ bond lengths should decrease by ∼5 pm upon oxidation. This leads to a reduced reorganization energy inside the protein (Table 6). As for the rubredoxins, the individual values vary quite a lot, 37−52 kJ/mol, but both estimates are appreciably lower than in a vacuum (75 kJ/mol). On average (44 kJ/mol), the reorganization energy is almost halved in the protein. It is also notable that λ_{ox} is appreciably larger than λ_{red}. This is most likely caused by the large variation in the Fe−S bonds in the reduced site.

Finally, it should be noted that the ΔE_1 values (also included in Table 5), i.e., the cost of changing the energy of the iron site from the vacuum geometry to the one in the protein, are quite large for the [2Fe−2S] ferredoxin models, 43−110 kJ/mol. This is larger than the corresponding values for rubredoxin, 14−38 kJ/mol (Table 3), and also for the blue copper proteins and alcohol dehydrogenase (30−70 kJ/mol).[24,39,68−70] This is probably an effect of the large charge of the cluster and the many polar interactions in the protein. ΔE_1 can be interpreted as the strain energy of the cluster when it is bound to the protein. It includes, however, several terms normally not considered as protein strain.[59] Interestingly, ΔE_1 is larger for the native protein structure (i.e., the oxidized site in the oxidized structure and vice versa); the opposite is normally found.[24] ΔE_1 can be expected to decrease if the protein is allowed to relax, typically by 5−20 kJ/mol.[24]

All energies presented until now are those directly obtained from the B3LYP low-spin calculations (the "broken-symmetry" solutions[9,10]). As discussed in Methods, this solution is not a pure spin state. Instead, the energy of the pure-spin ground state can be obtained by an extrapolation from this energy using also the properties of the high-spin wave function at the same geometry (eqs 3−7).[9,10,13] In Figure 3 we compare the Fe−Fe potential surface of the pure-spin and broken-symmetry states. It can be seen that the difference is quite small, less than 4 kJ/mol for all investigated distances (260−310 pm). Yet, spin coupling systematically favors shorter Fe−Fe distances in both oxidation states. Therefore, the optimum Fe−Fe distance is

(64) Teo, B.-K.; Shulman, R. G.; Brow, G. S.; Meixner, A. E. *J. Am. Chem. Soc.* **1979**, *90*, 5624−5631.
(65) Farrar, J. A.; Neese, F.; Lappalainen, P.; Kroneck, P. M. H.; Saraste, M.; Zumft, W. G.; Thomson, A. J. *J. Am. Chem. Soc.* **1996**, *118*, 11501−11514.
(66) Gamelin, D. R.; Randall, D. W.; Hay, M. T.; Houser, R. P.; Mulder, T. C.; Canters, G. W.; de Vries, S.; Tolman, W. B.; Lu, Y.; Solomon, E. I. *J. Am. Chem. Soc.* **1998**, *120*, 5246−5263.
(67) Larsson, S.; Källebring, B.; Wittung, P.; Malmström, B. G. *Proc. Natl. Acad. Sci. U.S.A.* **1995**, *92*, 7167−7171.
(68) Ryde, U.; Hemmingsen, L. *J. Biol. Inorg. Chem.* **1997**, *2*, 567−579
(69) Ryde, U. *Protein Sci.* **1995**, *4*, 1124−1132
(70) Ryde, U. *Eur. J. Biophys.* **1996**, *24*, 213−221.

Table 7. Geometries and Inner-Sphere Reorganization Energies (kJ/mol) for the Rieske $(SCH_3)_2FeS_2Fe(Im)_2$ Models Calculated by the B3LYP Method, Both at the Low-Spin (in Accordance with Experiments) and High-Spin States[a]

oxidation state	system	λ, kJ/mol	distance to Fe (pm)			
			S_{Cys}	S_i	N_{His}	Fe
II + III	vacuum	18.3	233−239	225−229	216−220	271
	protein crystals		222−231	223−235	213−223	271
	vacuum, high spin	39.1	234−240	229−233	216−219	261
III + III	vacuum	21.8	227−232	219−230	210−212	275
	vacuum, high spin	43.0	227−231	222−239	211−212	293

[a] Experimental results have also been included.[71,72]

reduced by 4 pm in the oxidized state and by 6 pm in the mixed-valence state. This makes the distances closer to those found in experiments (cf. Table 5), even if the discrepancy is still 10−15 pm, corresponding to an energy cost of 1−5 kJ/mol.

Moreover, we have estimated the effect of spin coupling on the reorganization energies. From Table 6, it can be seen that the effect in most cases is small, 1−3 kJ/mol. However, for the two mixed-valence calculations in the protein, the effect is larger, 6−12 kJ/mol, but with a varying sign. This can be traced back to the electron delocalization parameter (*B*). This parameter can be estimated together with the Heisenberg spin coupling parameters (*J*) from eqs 3−6. The Heisenberg spin coupling parameters for the oxidized state, J_{ox}, are 252−381 cm^{-1}, in excellent agreement with experimental estimates (298−364 cm^{-1}) but less than half as large as earlier quantum chemical estimates (763−868 cm^{-1}) obtained with other, less accurate functionals.[15] However, the electron delocalization parameters for the mixed-valence state, 1900−2200 cm^{-1}, are much larger than in earlier calculations (394−912 cm^{-1}).[15] This overestimation propagates to the Heisenberg spin coupling parameters, J_{red}, which also are too large (1140−1260 cm^{-1}) compared both to experiments (196 cm^{-1}) and to other calculations (514−504 cm^{-1}).[15] If the *B*-factor contribution to J_{red} is ignored, the results are only slightly smaller than experiments, 139−186 cm^{-1}. This indicates that the method to estimate the *B* factor from orbital energy differences does not work properly for these systems without symmetry. Therefore, and also because of the small effect of spin coupling observed in most systems, we decided to ignore this effect for the other spin-coupled systems.

Finally, it should be mentioned that we have also studied the fully reduced $(SCH_3)_2FeS_2Fe(SCH_3)_2^{4-}$ complex. However, the large negative charge of this complex makes it unstable in a vacuum: Two of the cysteine models dissociate from the iron ions when it is optimized in a vacuum.

Rieske Site. In the electron-transport chain of chloroplasts and mitochondria, binuclear iron−sulfur clusters are found with unusually high reduction potentials (cf. Table 1). These so-called Rieske centers are [2Fe−2S] ferredoxins with the cysteine ligands of one of the iron ions replaced by two histidine ligands. In the reduced state ($Fe^{II}Fe^{III}$), the extra electron resides on iron ions with two histidine ligands, whereas it alternates between the two ions in the normal ferredoxins.[5] This is reproduced in our calculations. We have modeled these sites by $(SCH_3)_2FeS_2Fe(Im)_2^{0/-}$. The optimized structures are shown in Table 7. All distances around the iron ions are shorter than in $Fe_2S_2(SCH_3)_4$, the Fe−Fe distance by 10 and 28 pm, the Fe−S_{Cys} distances by 2 and 6 pm, and the average Fe−S_i distances by 7 and 9 pm, for the oxidized and mixed-valence states, respectively. This is probably an effect of the smaller net charge (−1 and 0) of the Rieske models. The Fe−N distances are 211 and 218 pm, respectively.

There are two crystal structures available for Rieske centers, one from mitochondria and one from chloroplasts.[71,72] Both are in the mixed-valence (reduced) state. As can be seen from Table 7, the calculated Fe−S_{Cys} bond lengths are too long by 8−11 pm (as an effect of deficiencies in the B3LYP method and protein solvation effects), whereas the Fe−S_i and Fe−N bonds lengths are close to the experimental averages. The Fe−Fe bond length is exactly the same as in the two crystal structures, 271 pm, which of course is a lucky coincidence, considering the low resolution of the structures and the flexibility of this bond.

Upon oxidation, the Fe−S_{Cys} and Fe−N distances of the Rieske model decrease by ∼7 pm, whereas the Fe−Fe distance increases by 4 pm. As in the [2Fe−2S] ferredoxin model, the Fe−S_i distances decrease slightly for the iron ion that is not oxidized (by 1−2 pm), whereas the distances to the other iron ion increase by 7−8 pm. However, contrary to what was found for the former system, the Fe−S_i distances are quite similar in the mixed-valence state, 225−229, whereas they are distinctly dissimilar in the oxidized state (230 pm for the iron ion bound to the thiolate groups and 219 pm for the other iron ion). This is of course an effect of the ligand substitution.

Interestingly, the inner-sphere reorganization energy of the Rieske model, 40 kJ/mol, is appreciably lower than for the ferredoxin model and similar to that of the rubredoxin model. The reason for this is that the change in all iron−ligand distances is quite small, <8 pm, i.e., less than in the rubredoxin model.

Recently, it has been suggested that theoretical calculations of antiferromagnetically coupled polynuclear metal complexes often can be done in the ferromagnetically coupled high-spin state (which is computationally more simple).[73,74] Therefore, we have also calculated structures and reorganization energies of the [2Fe−2S] ferredoxin and Rieske models in the high-spin states (with 9 or 10 unpaired electrons). The results in Tables 5−7 show appreciable differences compared to the low-spin calculations. Even if the distances to the terminal ligands do not differ by more than 1 pm, the Fe−S_i bond lengths may change by up to 9 pm and the flexible Fe−Fe distances by as much as 18 pm. For the Rieske site, the Fe−S_i bonds lengthen in the high-spin state, whereas in the ferredoxin model they both increase and decrease, giving a smaller variation in the reduced state but a larger one in the mixed-valence state.

Most importantly, these changes in geometry have large effects on the reorganization energy. As can be seen in Tables 6 and 7, the reorganization energy of the ferredoxin model in the high-spin state is decreased by 18 kJ/mol to 59 kJ/mol, whereas it is more than doubled for the Rieske model, to 82 kJ/mol. Thus, for geometries and reorganization energies, it is not a good idea to use high-spin models, at least for iron−sulfur clusters.

[4Fe−4S] Ferredoxin Site. Next, we studied three oxidation states of $Fe_4S_4(SCH_3)_4$ as a model of the [4Fe−S] ferredoxin site. The optimized structures are described in Table 8. As expected, they are slightly distorted cubes (cf. Figure 4). Compared to the [2Fe−2S] sites, the Fe−S_{Cys} distances are consistently shorter; the average Fe−S_{Cys} bond lengths in the three oxidation states are 239, 232, and 226 pm compared to 247 and 236 pm in the two $Fe_2S_2(SCH_3)_4$ complexes. The Fe−

(71) Iwata, S.; Saynovits, M.; Link, T. A.; Michel, H. *Structure* **1996**, *4*, 567.
(72) Carrell, C. J.; Zhang, H.; Cramer, W. A.; Smith, J. L. *Structure* **1997**, *5*, 1613.
(73) Pavlov, M.; Blomberg, M. R. A.; Siegbahn, P. E. M. *Int. J. Quantum Chem.* **1999**, *73*, 197−207.
(74) Siegbahn, P. E. M.; Westerberg, J.; Svensson, M.; Carbtree, R. H. *J. Phys. Chem.* **1998**, *B102*, 1615−1623.

Table 8. Geometries and Inner-Sphere Reorganization Energies (λ) for the $Fe_4S_4(SCH_3)_4$ Ferredoxin Models Calculated by the B3LYP Method[a]

oxidation state	system	λ, kJ/mol	distance to Fe (pm)		
			S_{Cys}	S_i	Fe
II_3III_1	vacuum	32.7	237−241	233−246	277−322
	models		228−231	227−237	271−281
	protein crystals		228−232	226−232	254−270
	protein EXAFS		226		271
II_2III_2	vacuum	$\lambda_{red} = 29.2$ $\lambda_{ox} = 18.3$	232−233	234−237	282−293
	models		224−229	223−233	270−279
	protein crystals		213−233	214−240	256−279
	protein EXAFS		225		266−273
II_1III_3	vacuum	24.8	226−227	227−240	284−310
	models		220−221	223−228	274[b]
	protein crystals		218−226	215−237	267
	protein EXAFS		226		274

[a] Experimental results for model complexes[61,62,75−80] as well as proteins (both crystal structures[81,83] and EXAFS data[64]) have also been included when available. [b] Average distance.

S_i and Fe−Fe distances are similar to those found in the dimeric sites, but they vary quite a lot within the cuboidal sites.

Crystallographically characterized inorganic models and protein crystal structures are available for all three oxidation states.[61,62,64,75−83] Their structures are included in Table 8. It can be seen that our calculated models have 4−12 pm too long Fe−S bonds and 6−41 pm too long Fe−Fe bonds. Probably, all distances will be shorter in the protein, as an effect of the hydrogen bonds present there (typically eight to the S_{Cys} and three to the S_i atoms[81]).

As in the inorganic model systems, the calculated distances can be divided into two or three groups representing distances within or between Fe_2S_2 dimer planes (with the same or different oxidation state). For example, in the $Fe^{II}_2Fe^{III}_2$ state, the eight Fe−S_i distances within the two mixed-valence Fe_2S_2 pairs are longer, ∼237 pm, than those between the two planes, 234 pm. In the model systems, the difference is similar, 3−6 pm.[76] The same is true for the Fe−Fe distances; the four between the planes are shorter than the two within the planes, 282 and 293 pm, respectively. In the models, the same trend is present, but the difference is smaller.[76,82]

For the reduced cluster, model compounds show large variation in the structure, ranging from compressed to elongated sites.[75−78] This indicates that it is highly plastic.[5,55] Our optimized structure is similar to two of the observed structures, with four short bonds within the mixed-valence Fe_2S_2 pair, four long bonds within the reduced Fe_2S_2 pair, and two short and two long distances between the two pairs. Of course, such a clear distinction between the two Fe_2S_2 pairs can only be seen if the extra electron is localized on one pair, which is unlikely in models and proteins.[84,85] This may explain why our structures show a larger variation in the bond lengths than the experimental ones.

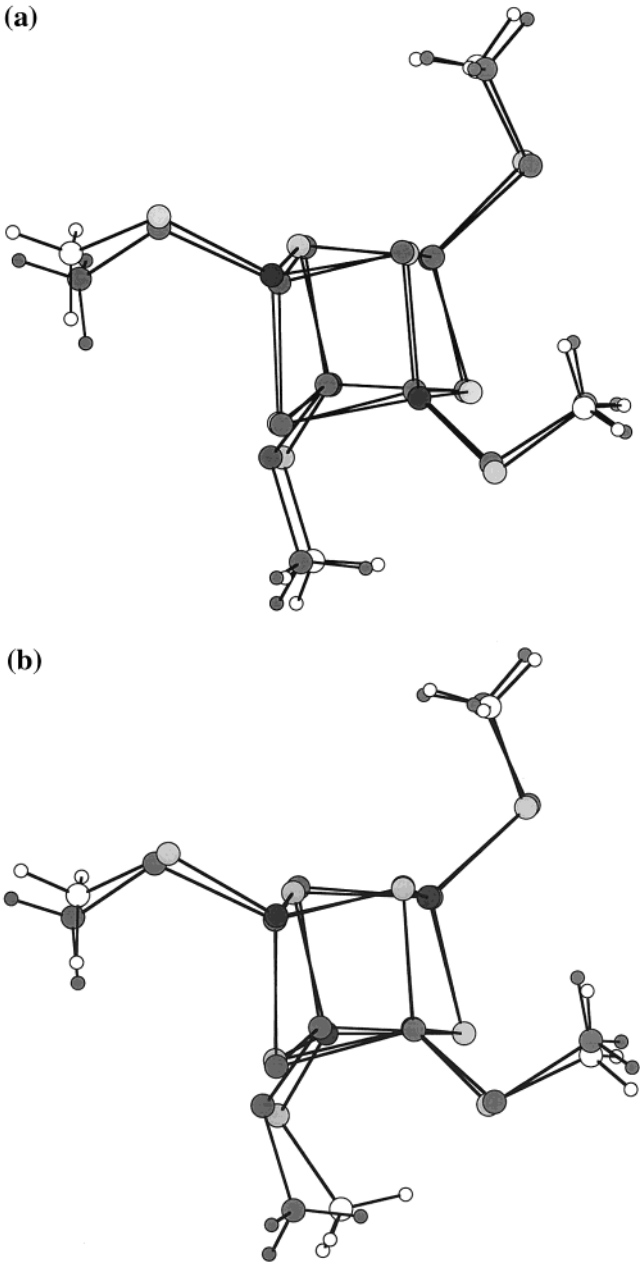

Figure 4. Difference in geometry (a) between the $Fe^{II}_3Fe^{III}$ and $Fe^{II}_2Fe^{III}_2$ (shaded) forms and (b) between the $Fe^{II}_2Fe^{III}_2$ (shaded) and $Fe^{II}Fe^{III}_3$ forms of the [4Fe−4S] ferredoxin model $Fe_4S_4(SCH_3)_4$.

When the $Fe^{II}_3Fe^{III}$ site is oxidized, several changes are seen (cf. Figure 4a). The Fe−S_{Cys} bonds contract by 5−8 pm (most for the reduced Fe_2S_2 pair), and the Fe−S_i distances within the reduced Fe_2S_2 pair decrease by 9 pm, whereas those of the mixed-valence pair hardly change at all. Two of the Fe−S_i bonds between the pairs decrease by 8 pm, whereas the other two increase by 1 pm. Thus, six Fe−S bonds change by the same amount as in the rubredoxin site (where there are only four bonds). Therefore, the reorganization energy is slightly larger than this site, 62 kJ/mol.

(75) Laskowski, E. J.; Frankel, R. B.; Gilum, W. O.; Papaefthymiou, G. C.; Renaud, J.; Ibers, J. A.; Holm, R. H. *J. Am. Chem. Soc.* **1978**, *100*, 5322−5337.
(76) Berg, J. M.; Hodgson, K. O.; Holm, R. H. *J. Am. Chem. Soc.* **1979**, *101*, 4586−4593.
(77) Stephans, D. W.; Papaefthymiou, G. C.; Frankel, R. B.; Holm, R. H. *Inorg. Chem.* **1983**, *22*, 1550−1557.
(78) Hagen, K. S.; Watson, A. D.; Holm, R. H. *Inorg. Chem.* **1984**, *23*, 2984−2990.
(79) Marscharak, P. K.; Hagen, K. S.; Spence, J. T.; Holm, R. H. *Inorg. Chim. Acta* **1983**, *80*, 157−170.
(80) O'Sullivan, T. M.; Millar, M. *J. Am. Chem. Soc.* **1985**, *107*, 4096−4097.
(81) Dauter, Z.; Wilson, K. S.; Sieker, L. C.; Meyer, J.; Moulis, J.-M. *Biochemistry* **1997**, *36*, 16065−16073.
(82) Que, L.; Bobrik, M. A.; Ibers, J. A.; Holm, R. H. *J. Am. Chem. Soc.* **1974**, *96*, 4168−4178.
(83) Brookhaven Protein Data Bank files: 1fca, 1fdb, 1fdc, 1hip, and 1isu.
(84) Beinert, H. *J. Biol. Inorg. Chem.* **2000**, *5*, 2−15.
(85) Dilg, A. W. E.; Mincione, G.; Achterhold, K.; Iakovleva, O.; Mentler, M.; Luchinat, C.; Bertini, I.; Parak, F. G. *J. Biol. Inorg. Chem.* **1999**, *4*, 727−741.

Table 9. Geometries and Inner-Sphere Reorganization Energies for Some Iron Models Related to Desulfoferrodoxin Calculated by the B3LYP Method[a]

			distance to Fe (pm)				
model	oxidation state	λ_i, kJ/mol	L_1	L_2	L_3	L_4	L_5
$Fe(Im)_4(SCH_3)$	II	21.7	218	218	229	230	234
	III	20.1	213	213	217	217	226
protein crystal[88]	III		206	211	220	221	229
$Fe(Im)_4$	II	23.1	208	208	208	208	
	III	23.8	200	200	200	200	
$Fe(Im)_3(SCH_3)$	II	24.0	204	204	205	223	
	III	25.5	211	211	211	228	
$Fe(Im)_2(SCH_3)_2$	II	22.9	216	217	232	232	
	III	24.1	207	208	224	224	
$Fe(Im)(SCH_3)_3$	II	21.5	221	236	236	239	
	III	25.3	212	227	228	228	

[a] All complexes were studied in the high-spin state. The order of the L_1-L_4 ligands is the same as in the model formula.

When the complex is further oxidized to the $Fe^{II}Fe^{III}_3$ state, changes in the geometry are smaller (see Figure 4b). All $Fe-S_{Cys}$ bonds decrease by 6 pm, whereas most $Fe-S_i$ bonds lengths change by less than 1 pm. Only two bonds within a pair increase by 3 pm and two bonds between the pairs decrease by 7 pm. All these changes are less than in the rubredoxin site. Therefore, it is somewhat unexpected that the reorganization energy is slightly larger than the energy for that site, 43 kJ/mol (even considering that there are 4 times as many Fe−S bonds in the [4Fe−4S] site). The reason is probably that there are quite substantial changes in the Fe_4S_4 core structure, as is flagged by a 28 pm increase in two of the Fe−Fe bonds. Compared to inorganic models, the calculated changes seem to be reasonable for the average $Fe-S_i$ distances (2 pm) but slightly too large for the $Fe-S_{Cys}$ bonds (4 pm).[80]

Holm and co-workers have estimated the total self-exchange reorganization energy ($\lambda_i + \lambda_o$) for the $Fe^{II}_3Fe^{III}-Fe^{II}_2Fe^{III}_2$ couple of the $Fe_4S_4(SC_6H_4CH_3)_4$ model compound to be 146 kJ/mol.[57] They also estimated the inner-sphere part from the observed changes in the Fe−S bonds and the corresponding frequencies to be 32 kJ/mol. The latter estimate is half as large as ours probably because we have not included the protein in our calculations.

Similarly, the total self-exchange reorganization energy of a high-potential iron protein has been estimated to be 70−90 kJ/mol.[86] This result is in accordance with our calculations, provided that the outer-sphere contribution of this protein is similar to that of plastocyanin (a protein of a similar size), ~40 kJ/mol,[87] and that the reorganization energy of the HiPIP model inside the protein is approximately half of the vacuum estimate, as was observed for the rubredoxin and [2Fe−2S] ferredoxin models, as well as for blue copper proteins.[24]

Desulfoferrodoxin Site. Recently, it has been shown that desulfoferrodoxin contains an iron site with only one cysteine and four histidine ligands.[88] We have modeled this site by $Fe(Im)_4(SCH_3)^{+/2+}$. As can be seen in Table 9, the optimized structures have two short and two long $Fe-N_{His}$ bonds due to $CH\cdots S_{Cys}$ hydrogen bonds. The bond lengths in the oxidized structure are close to those in the crystal structure of desulfoferrodoxin; the average Fe−N distance is 215 pm in both structures, whereas our calculated $Fe-S_{Cys}$ distance is 3 pm shorter than in the crystal structure. The reorganization energy of the desulfoferrodoxin model is close to that of rubredoxin, 42 kJ/mol.

Table 10. Geometries and Inner-Sphere Reorganization Energies (kJ/mol) for Some Four- and Six-Coordinate Iron Models Calculated by the B3LYP Method[a]

			distance to Fe (pm)			
model	oxidation state	λ_i, kJ/mol	L_1	L_2	L_3	L_4
$Fe(H_2O)_6$	II	30.5	215	215	215	215
	III	34.9	205	205	205	205
$Fe(H_2O)_4$	II	35.9	204	204	204	204
	III	29.9	196	196	196	196
$Fe(NH_3)_4$	II	8.0	214	214	214	214
	III	9.5	209	209	209	209

[a] All complexes were assumed to be high spin. The order of the L_1-L_4 ligands is the same as in the chemical formula for the model. For $Fe(H_2O)_6$, all six distances are the same, so only four are given.

This indicates that imidazole and cysteine give rise to sites with similar electron-transfer properties. Therefore, we studied the five models of the type $Fe(Im)_n(SCH_3)_{4-n}$, with $n = 0-4$ ($n = 0$ gives the rubredoxin site). The results are also included in Table 9 and show that the reorganization energy varies between 40 and 49 kJ/mol. It is lowest for the rubredoxin site, whereas the other four sites all have a reorganization energy around 47 kJ/mol. Interestingly, the $Fe-S_{Cys}$ bonds change more during oxidation than the $Fe-N_{His}$ bonds. This indicates that the latter bond is stiffer, although the $Fe-S_{Cys}$ bond involves an interaction between two oppositely charged ions. This is confirmed by direct calculations of the corresponding force constants, which are 0.027 and 0.038 kJ mol^{-1} pm^{-2} for the Fe−N bonds in $Fe(Im)_4^{2+/3+}$ but 0.017 and 0.032 kJ mol^{-1} pm^{-2} for the Fe−S bonds in $Fe(SCH_3)_4^{2-/1-}$.

Thus, in terms of reorganization energy, cysteine and histidine can be used almost interchangeably. However, cysteine has the advantage of stabilizing a low coordination number for both oxidation states (because of its negative charge and bulkiness), whereas higher coordination numbers are preferred with the uncharged histidine ligands. Moreover, cysteine forms more covalent bonds and therefore a better path for electron transfer. This can be seen from the higher spin densities on the cysteine models than on the imidazoles (e.g., 0.10 e compared to 0.05 e for the reduced $Fe(SCH_3)_4$ and $Fe(Im)_4$ complexes and 0.30 e compared to 0.20 e for the oxidized complexes).

Comparison with the Blue Copper Proteins. We have shown that the inner-sphere reorganization energy of six types of iron−sulfur clusters is similar to those found for the blue copper proteins and the binuclear Cu_A site, both in a vacuum (43−90 kJ/mol[22−24]) and in the proteins (27−38 kJ/mol[24]). It is instructive to compare how the two types of sites have achieved such a low reorganization energy. The blue copper proteins reduce their reorganization energy by using ligands with a small force constant for the bond to copper (methionine) and by using ligands that give structures that are similar to those for Cu(I) and Cu(II) (cysteine).[22] The Cu_A site has a delocalized electron in the mixed-valence state, which reduces the force constants and the change in the metal−ligand bond lengths upon reduction.[23]

To examine how the iron−sulfur clusters have achieved a low reorganization energy, we examine an iron ion in aqueous solution, modeled by $Fe(H_2O)_6$. As can be seen in Table 10, this complex has an inner-sphere reorganization energy of 65 kJ/mol. This is actually slightly less than for the [2Fe−2S] site. However, the outer-sphere component is large in aqueous

(86) Babini, E.; Bertini, I.; Borsari, M.; Capozzi, F.; Luchinat, C.; Zhang, X.; Moura, G. L. C.; Kurnikov, I. V.; Beratan, D. N.; Ponce, A.; Di Bilio, A. J.; Winkler, J. R.; Gray, H. B. *J. Am. Chem. Soc.* **2000**, *122*, 4532.

(87) Soriano, G.M.; Cramer, W. A.; Krishtalik, L. I. *Biopys. J.* **1997**, *73*, 265.

(88) Coelho, A. V.; Matias, P.; Fülöp, V.; Thompson, A.; Gonzalez, A.; Carrondo, M. A. *J. Biol. Inorg. Chem.* **1997**, *2*, 680−689.

solution, giving a total reorganization energy of ∼250 kJ/mol.[89,90] The reorganization energy of the corresponding copper complex is more than 5 times larger (336 kJ/mol)[22] because Cu(I) assumes a lower coordination number than Cu(II). Yet, even if Cu(I) is forced to have the same coordination number and geometry as Cu(II), the reorganization energy is still twice as large as for iron (112 kJ/mol)[22] because the changes in the metal−ligand bond distances are larger: 24 pm for four bonds and 3 pm for two bonds for copper (Cu^{2+} is Jahn−Teller distorted) compared to 10 pm for all bonds in the iron complex.

Both the iron−sulfur clusters and the blue copper proteins are four-coordinate. Therefore, we studied the $Fe(H_2O)_4$ system. The reorganization energy of this complex is almost identical to that of the six-coordinate complex, 66 kJ/mol. This is an effect of a smaller change in the bond lengths (8 pm) and a lower number of bonds combined with more stiff bonds. The geometry is tetrahedral for both oxidation states. This is in strong contrast to copper, for which Cu(I) forms a tetrahedral complex, whereas Cu(II) assumes a square-planar structure. Therefore, the reorganization energy of copper (136 kJ/mol) is almost 3 times higher than for iron.[22]

The situation is similar for the $Fe(NH_3)_4$ complex. It has a very low reorganization energy of only 18 kJ/mol, which is more than 7 times lower than for copper (122 kJ/mol). Thus, such a complex would constitute an excellent electron-transfer site. However, four neutral ligands do not form stable complexes with Fe(III), and amine ligands are not available in most proteins (the functional group of lysine has an acid constant that is too large and is therefore protonated at normal pH values). Instead, cysteine ligands are needed to lower the coordination number and give a favorable electron-transfer path, whereas histidine could be used instead of ammonia (but with higher reorganization energies, as we saw in the preceding section).

Thus, we can conclude that iron a priori is a much better electron-transfer ion than copper because the two oxidation states of iron have the same preferences in coordination number and geometry. Moreover, the iron−sulfur clusters, like the blue copper proteins, employ nitrogen and sulfur ligands rather than oxygen ligands to reduce the metal−ligand force constants and therefore the reorganization energy. This is a general rule that has also been observed experimentally.[91] However, after this, it seems that the actual choice of iron ligands is determined more by practical reasons (e.g., that the metal should bind strongly to the protein) and by the need for obtaining a proper electronic path rather than by considerations of the reorganization energy. Similarly, the choice of the type of iron−sulfur cluster (i.e., the number of iron ions and the type of ligands) seems to be mainly a question of stability and reduction potential. A large cluster may decrease the distance of electron transfer,[65] may allow the site to be more buried in the protein, and may give a directionality for electron transfer.[56,92] This may explain why the polynuclear iron−sulfur clusters are more common than the rubredoxin site.

Acknowledgment. This investigation was supported by grants from the Swedish Natural Science Research Council (NFR). It was also supported by computer resources of the Swedish Council for Planning and Coordination of Research (FRN), Parallelldatorcentrum (PDC) at the Royal Institute of Technology, Stockholm, the High Performance Computing Center North (HPC2N) at the University of Umeå, and Lunarc at Lund university.

IC000752U

(89) Silverman, J.; Dodson, R. W. *J. Phys. Chem.* **1952**, *56*, 846.
(90) Brunschwig, B. S.; Logan, J.; Newton, M. D.; Sutin, N. *J. Am. Chem. Soc.* **1980**, *102*, 5798.
(91) LeCloux, D. D.; Barrios, A. M.; Mizoguchi, T. J.; Lippard, S. J. *J. Am. Chem. Soc.* **1998**, *120*, 9001−9014.
(92) Randall, D. W.; Gamelin, D. R.; LaCroix, L. B.; Solomon, E. I. *J. Biol. Inorg. Chem.* **2000**, *5*, 16−29.